[Frontiers in Bioscience 11, 2623-2630, September 1, 2006]

Mutation of siRNA results in thermodynamically unstable duplex which influences knockdown of *dmrt1* by RNA interference

Kai Yao, Heng Lu, Hanhua Cheng and Rongjia Zhou

Department of Genetics and Center for Developmental Biology, College of Life Sciences, Wuhan University, Wuhan 430072, P. R. China

TABLE OF CONTENTS

1. ABSTRACT

MicroRNAs (miRNAs) constitute a growing class of non-coding RNAs that are thought to regulate gene expression by translational repression and mRNA degradation. We report here that short interfering RNA (siRNA) mutation significantly changed kinetics of the folding and unfolding of secondary structures and decreased *Tm* value of the duplex melting. The mutant duplex was more unstable thermodynamically than the normal structure. Furthermore negative effects of the mutation on RNA interference (RNAi) was observed in both mouse *dmrt1* transfected COS-7 and Sertoli cells in which endogenous *dmrt1* was expressed. However, interference efficiency of mutational and normal duplex in Sertoli cells was not significant in comparison with those in *dmrt1* transfected COS-7 cells, suggesting complex regulatory mechanisms in RNAi in endogenous *dmrt1* expression. Abundance of intronic miRNA structures observed in the *dmrt1* gene may also contribute to the precise regulation cascade in the *dmrt1* expression. These findings help in further understanding RNA silence in vertebrate development and drug design for target gene.

2. INTRODUCTION

Naturally occurring microRNAs (miRNAs) are 19- to 25-nt transcripts cleaved from 70- to 100-nt hairpin precursors, and are encoded in the genomes of invertebrates, vertebrates and plants. miRNAs are a growing family of small non-coding regulatory genes that regulate the expression by translational repression and mRNA degradation. The biological functions of miRNAs are not yet fully understood. However, they have been implicated in the control of cell proliferation and death, and in stress resistance and fat metabolism in flies (1, 2), insulin secretion, haematopoietic lineage differentiation, chronic lymphocytic leukemia and cancers in mammals (3-6), neuronal patterning in nematodes (7), morphogenesis in zebrafish (8) and leaf and flower development in plants (9), indicating that they could play important roles in many biological processes.

Hunting for miRNAs challenges the imagination. To date, the total number of human microRNAs is at least 800 based on recent report using an integrative approach combining bioinformatic predictions with microarray

analysis and sequence-directed cloning (10), which is much larger than previous estimate of 200-225 in vertebrates (11) or 321 (http://microrna.sanger.ac.uk). These findings indicate that microRNAs not only have important roles in the regulation of gene expression, but also may have a key role in the evolutionary process and in the evolved complexity of higher mammals because a substantial portion of miRNAs are primate-specific with specifically expression in developmental tissues. However, the function of the large majority of these miRNAs remains unclear.

Pre-miRNA precursors are processed into miRNAs or short interfering RNAs (siRNA) that mediate translational repression and mRNA degradation. The process is catalysed by dsRNA-specific RNase-III-type endonucleases, termed Drosha and Dicer, which contain catalytic RNase III and dsRNA-binding domains (dsRBDs, to bind the stem and defines the distance of the cleavages from the base) (12-17). Dicer contains another PAZ domain to bind to the 2 nt 3' overhang present at the base of the pre-miRNA hairpin, which is a crucial step of RNA interference (RNAi) (18, 19). miRNAs are transcribed as long primary transcripts, which are first processed by Drosha in the nucleus. When Drosha excises the fold-back miRNA precursor, a 5'phosphate and a 2-nucleotide 3'overhang remain at the base of the stem. The miRNA precursor is then exported to the cytoplasm by means of the nuclear export receptor, exportin-5, where it is further processed by Dicer into mature RNA duplexes of about 22 nucleotides in length, which — like Drosha-processing products — have 5' phosphates and 2-nucleotide 3'overhangs. miRNA-duplex-containing ribonucleoprotein particles (RNPs) are subsequently rearranged into the RNA induced silencing complex (RISC). The functional RNPs contain only single-stranded siRNAs or miRNAs. The assembly of RISC is ATP dependent (20, 21), which probably reflects the requirement for energy driven unwinding of the siRNA-duplex. Although RNA helicases may involve in the unwinding process, such as DEAD-box RNA helicase in *D. melanogaster* (22), the mechanisms for unwinding of the siRNA-duplex and for choosing which of the two strands enters the RISC are still waiting for answer.

The RISC identifies target messages based on perfect (or nearly perfect) complementarity between the siRNA and the mRNA, and then the endonuclease of the RISC cleaves the target mRNA. Because some miRNAs downregulate large numbers of target mRNAs (23), if unperfect complementarity occurs, exactly regulation of developmental processes by miRNAs remains unclear. We report here thermodynamic characteristics of siRNAs and their mutants targeting mouse *dmrt1* and the mutation affected knockdown effects of the gene by the RNA interference in both transfected cells and endogenous Sertoli cells. Furthermore intron-derived miRNAs within the *dmrt1* gene may be an alternative pathway for miRNA biogenesis in regulation of *dmrt1* expression. These findings will undoubtedly help in further understanding RNA silence in vertebrate development and drug design for target gene.

3. MATERIALS AND METHODS

3.1. UV melting profile

The denaturations were carried out on a Beckman DU-640 UV-vis spectrophotometer equipped with a digital circulating water bath. The absorbance of oligo(s) (in 2ml at 2 μmol/L) in annealing buffer (10 mmol/L Tris, 100 mmol/L NaCl, pH7.4) was monitored at 260 nm, while temperature was increased from 10 to 90 °C at a rate of about 0.5-1.5 °C/min. Melting profiles were analyzed by fitting them to a concerted two-state model in which the absorbance A is given by the following equations: $A=A_f\theta+A_u(1-\theta)$, $\theta=1/[1+e^{(\Delta H0/R)\ (1/T\ -1/Tm)}]$, ΔH^0: the van't Hoff enthalpy, and R: the gas constant (8.311 J mol^{-1} K^{-1}) (24, 25).

3.2. Real-time fluorescent melting curves

The fluorescence signal (F) was monitored continuously during the temperature ramp and then plotted against the temperature (T) using the multi-channel RotorGene 3000 (Corbett Research, Australia). Reactions were performed in a 25 μL mix containing 1x Sybr Green I, 0.16 μmol/L each oligo, 100 mmol/L NaCl and 10 mmol/L Tris, pH7.4. The reaction conditions were 5min at 94°C, then temperature was increased from 25 to 94°C at a rate of 1°C/min. These curves were transformed to derivative melting curves [(-dF/dT) vs T].

3.3. RNA isolation and cDNA synthesis

Transfected cells after forty eight hours were collected. Total RNAs (transfected cells and testis) were prepared by the RNeasy Mini kit (Qiagen, USA) according to the manufacture's instructions. All the RNAs were digested by RNase-free DNase I and purified. About 3ug RNAs were used as template for reverse transcription using 0.5ug $poly(T)_{20}$ primer and 200 U MMLV reverse transcriptase (Promega, USA).

3.4. RNAi clones

The siRNA included in the analysis were determined using Ambion online siRNA design tool (*www.ambion.com/techlib/misc/siRNA_design.html,*Ambion, Austin, TX, USA). Hairpin DNA sequences were synthesized as two complementary oligonucleotides, annealed, and ligated between the *Bbs*I and *Xba*I sites and replaced EGFP coding sequence of pmU6pro vector (a gift from David Turner) to generate interference vector pmdcdsi and mutant vector pmdcdsi-m. The sequences are 5'TTTGAAGAACTGGGTATCAGCCATGGGCTGATACCCAGTTCTTCTTTTT3' and 5'CTAGAAAAAGAAGAACTGGGTATCAGCCCATGGCTGATACCCAGTTCTT3'. Mutant sequence at 7 nt of target site (C-T) is 5'TTTGAAGAACTGGGTATCAGCCATGGGCTGATACCCATTTCTTCTTTTT3'.

3.5. Expression vector

Porcine dmrt1 promoter sequence was amplified with primers containing restriction sites for *Aat*II and *Sac*II respectively: 5'GCCGACGTCTGTAGTCTTGAATCCCTCCA3' and 5'GCACCGCGGTGCCCCAAGGAGAAGCG3'. PCR were performed in a 20 μL reaction mix containing 10 mmol/L Tris-HCl pH8.3, 1.5 mmol/L $MgCl_2$, 50 mmol/L

KCl, 150 mmol/L dNTP, 0.2 μmol/L each primer, 1 U Taq DNA polymerase. Amplification conditions were: 94°C, 40s; 67°C, 40s; 72°C, 2m30s for 35 cycles. A 2453 bp fragment was subcloned into pGEM-T Easy(Promega). Porcine *dmrt1* promoter was cut with *Aat*II and *Sac*II and subcloned into *Aat*II and *Sac*II sites upstream of the coding sequence for EGFP of pEGFP-N1 (Clontech). The EGFP coding sequence was then replaced by mouse *dmrt1* coding sequence to generate the dmrt1 expression vector.

Mouse *dmrt1* coding sequence (1145 bp) was obtained as follows. Testis cDNAs were amplified using *dmrt1* primers containing restriction sites for *Sac*II and *Not*I respectively:5'CGACCGCGGATGCCGAACGACGACACATT3' and 5'GATGCGGCCGCTCACTCGTCCTCATCCT3'. PCR was performed in a 20 μL reaction mix containing 10 mmol/L Tris-HCl pH8.3, 1.5 mmol/L $MgCl_2$, 50 mmol/L KCl, 150 mmol/L dNTP, 0.2 μmol/L each primer, 1 U Taq DNA polymerase. Amplification conditions were: 94°C, 30s; 66°C, 30s; 72°C, 1m10s for 35 cycles.

3.6. Cell preparation and transfection analysis

Cos-7 cells were grown in DMEM (GIBCO) supplemented with 10% fetus bovine serum (FBS). Primary Sertoli cells were prepared and cultured as described elsewhere (26). Briefly, testes were removed aseptically from 15-day-old mice, washed in PBS and decapsulated. The tissue was minced into 2- to 5-mm pieces and resuspended in PBS containing 0.25% trypsin (Sigma). 0.2% collagenase I (Sigma) was added and the suspension was vigorously shaken at 37°C. After 20-25min, the suspension was added DMEM/F-12 medium (GIBCO) with 20% FBS and blew repeatedly through a pipette. After the cluster of tissue was discarded, the suspension was centrifuged for 10min at 300g. The supernatant was then discarded and the cell aggregates were further dispersed. The cell pellet by low-speed centrifugation was washed three times with PBS, then transfered into the culture flask and feeded in DMEM/F-12 medium with 20%FBS at 37°C. For transient transfection, cos-7 cells and primary Sertoli cells were seeded onto 24-well plates at a density of 26000 cells/well. Transfections for cos-7 cells were performed with Lipofectamine 2000 (Invitrogen) as directed by the manufacturer. For cos-7 cells, 1 μg of *dmrt1* expression vector was cotransfected with 1μg of pmdcdsi, pmdcdsi-m or pcDNA3.0 as a control respectively. For primary Sertoli cells, transfections were performed with 1 μg of pmdcdsi or pmdcdsi-m respectively using Lipofectamine 2000.

3.7. Real time fluorescent quantitative RT-PCR

Real time RT PCR was used for quantification of the *dmrt1* expression from transfected cos-7 and primary Sertoli cells using the multichannel RotorGene 3000 (Corbett Research, Australia), according to the supplied protocol. PCR cycling conditions were: 5 min at 94°C; 40 cycles of 30 s at 94°C, 30 s at 66°C, and 20 s at 72°C in a 25μL reaction mix containing 1x Sybr Green I. The primer sequences are: 5'AGTCCCCGAGGCTGCCCAAA3' and 5'GTGGCTGATACCCAGTTCTTCTTC3' for *dmrt1* and 5'CCTGCTGGATTACATTAAAGCACT3' and 5'GTCAAGGGCATATCCAACAACAAA3' for *hprt*. Simultaneous detection of *hprt* gene was used to normalize *dmrt1* expression. For robustness issues, each sample was performed in triplicate at least. Data were analyzed by the software Rotor-gene version 4.6 and then plotted in Microsoft Excel.

3.8. Intron miRNA analysis

Intron sequences within mouse *dmrt1* genomic BAC clone AC132140 were used for search for repeat sequences, their secondary structures and possible complementary regions with *dmrt1* mRNA using local BLAST and GeneQuest 5.01progam of DNAStar software (DNASTAR, Inc.).

4. RESULTS

4.1. Mutation changes kinetics of the folding and unfolding of secondary structures

The binding groove of the PAZ domain of the Dicer accommodates RNA of 5–7 nucleotides in length that forms a stable 1:1 complex (18). To realize the characteristic of the stem-loop duplex relative to binding by the Drosha and Dicer, a 43-mer oligonucleotide and its mutant (C-T) at 7-nt (last site) of target match, which may fold into a stem-loop duplex, were used to compare folding and unfolding kinetics of secondary structures. Mouse *dmrt1*, a transcription factor involving gonad development, was used as the target by the RNA interference. Figure 1 shows the folding and unfolding curves of the secondary structures. In reaction mix, there are two kinds of secondary structures for a duplex, intra-strand and inter-strand. When a C-T mutant at 7-nt was introduced (Figure 1A), two-"S" form of curve was observed, and folding-unfolding curve was significantly changed in comparison with the non-mutant (Figure 1B).

4.2. Mutation decreases *Tm* value of the duplex melting

Processing of dsRNAs by Dicer yields RNA duplexes of about 22 nucleotides in length without stem-loop. Two complementary oligos and relevant mutant (C-T) at 7-nt of target match were used to analyze their melting characteristic. Figure 2 shows the melting curves when temperature increased from 25 to 94°C. Mutation decreased *Tm* value of the duplex melting for 10.27 °C in comparison with non-mutant (Figure 2A,B). Analysis using real-time fluorescent melting curves verified further the *Tm* value decrease in the mutant duplex (Figure 3). Relevant absorbance value ratios of binding (Af) / unbinding (Au) were 1.20 for non-mutant and 0.85 for the mutant. These results suggested the mutant duplex was more unstable thermodynamically than the normal structure.

4.3. Mutation of siRNA influences knockdown of *dmrt1*

We constructed RNAi vector in which siRNA targeting mouse *dmrt1* mRNA was controlled by U6 promoter (Figure 4). The same mutant (C-T) at 7-nt of target match were introduced to study its knockdown efficiency in *dmrt1* transfected COS-7 and Sertoli cells

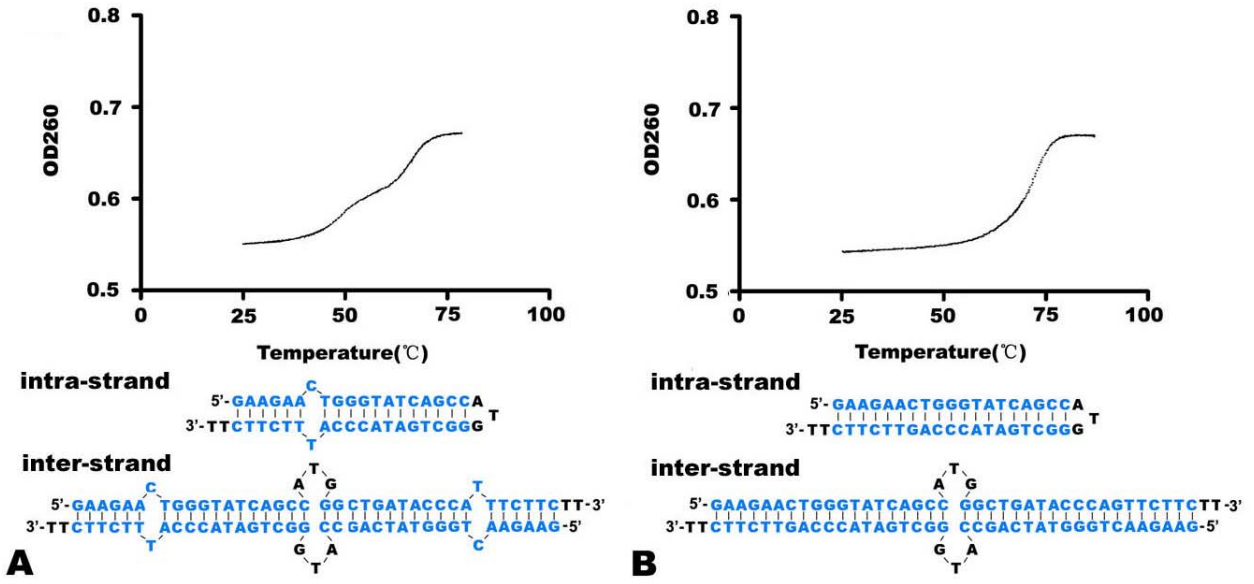

Figure 1. UV-melting profiles of a 43-mer oligonucleotide (B) and its mutant (C-T) at 7-nt (A). Denaturations were carried out on a Beckman DU-640 UV-vis spectrophotometer equipped with a digital circulating water bath. Melting profiles were analyzed by fitting them to a concerted two-state model as shown in materials and methods section. Lower panels show two forms of folding structures.

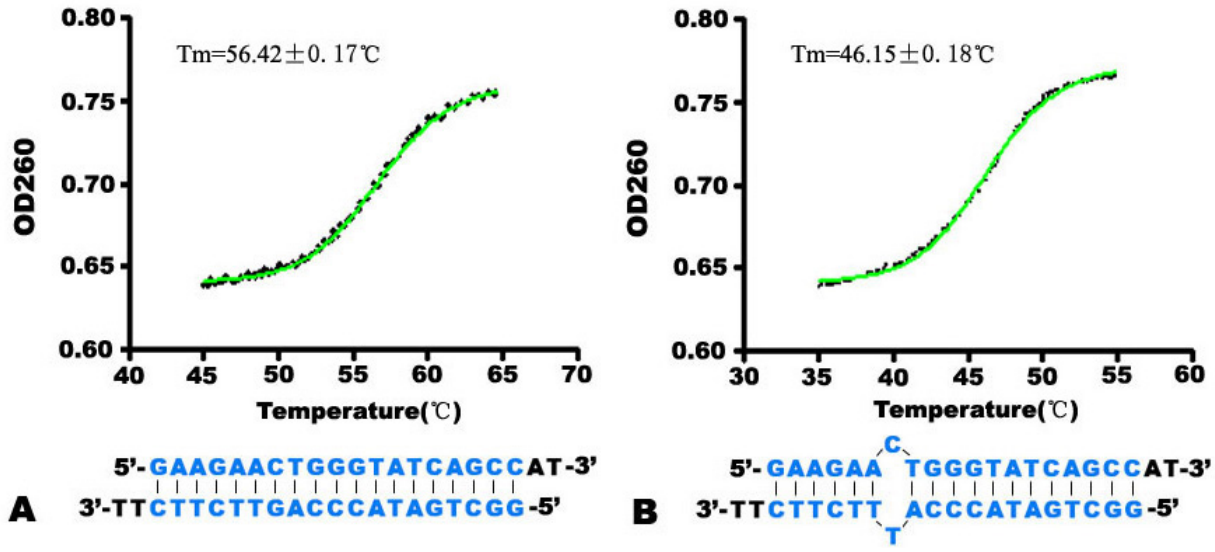

Figure 2. UV-melting profiles of two complementary oligonucleotides (A) and its mutant (C-T) at 7-nt (B). Melting curves were analyzed as in Figure 1. The *Tm* value decreased from 56.42 °C to 46.15 °C when mutation was introduced. Lower panels show the two complementary oligonucleotides.

in which endogenous *dmrt1* is expressed. Results using real-time fluorescent quantitative RT-PCR showed that RNA interference against *dmrt1* was obvious in both COS-7 (Figure 5A, 65%) and Sertoli cells (Figure 5B, 45%).Mutation at 7-nt affected significantly RNA interference against *dmrt1* in COS-7 (Figure 5A, 97%) and Sertoli cells (Figure 5B, 84%). However, interference efficiency of both mutational and normal duplex in Sertoli cells (endogenous *dmrt1* expressed) were not significant in comparison with those in *dmrt1* transfected COS-7 cells, suggesting more complex regulatory mechanisms in RNAi in endogenous *dmrt1* expression circumstance.

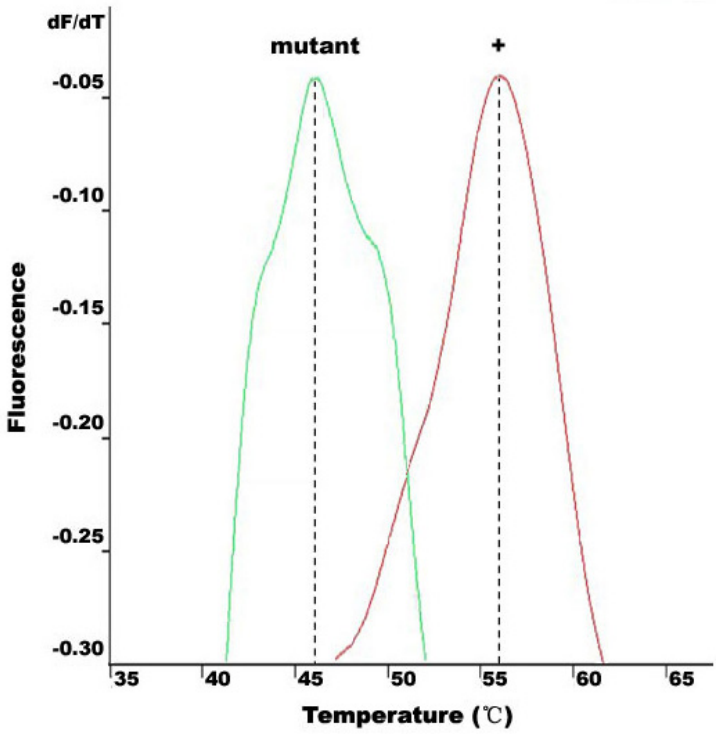

Figure 3. Real-time fluorescent melting curves. The fluorescence signal (F) was monitored continuously when the temperature increased from 25 to 94°C at a rate of 1°C/min and then plotted against the temperature (T) using the multi-channel RotorGene 3000. Curves were transformed to derivative melting curves [(-dF/dT) vs T]. Left curve is from mutant 5'GAAGAACTGGGTATCAGCC-3', and right from normal oligonucleotide 5'GAAGAACTGGGTATCAGCC3'.

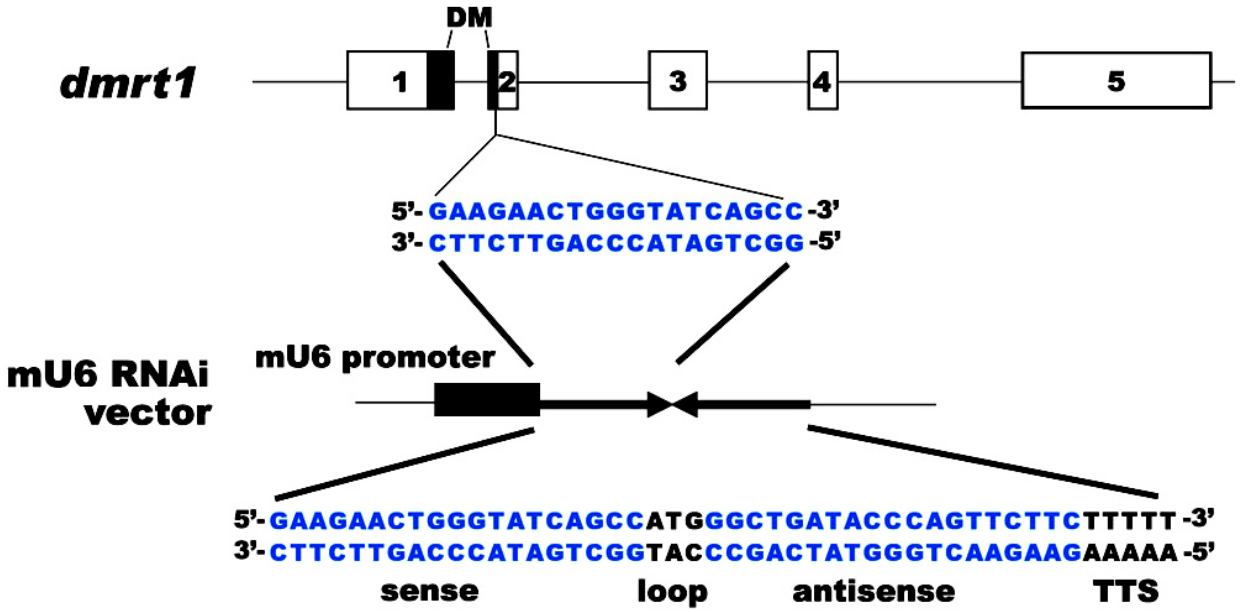

Figure 4. Mouse *dmrt1* genomic structure and its RNAi vector. Target sequence was at 3' region of the DM domain. Exons are boxed and the lines indicate the introns. Sense, loop and antisense indicate the sense, loop and antisense of hairpin RNA respectively. TTS, terminal termination signal. Hairpin RNA duplex was controlled by the U6 promoter.

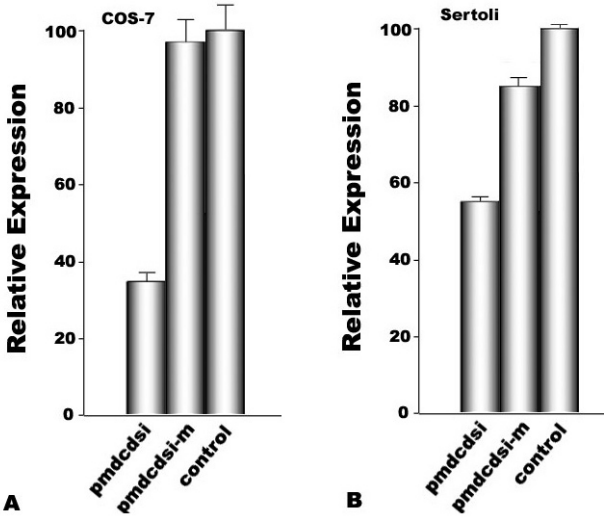

Figure 5. Real time fluorescent quantitative RT-PCR of *dmrt1* in transfected COS-7 (A) and primary Sertoli cells (B) when RNA interference vector (pmdcdsi) or its mutant (pmdcdsi-m) cotransfected respectively. The relative expression of *dmrt1* to *hprt* analyzed by real time fluorescent quantitative RT-PCR. Controls are without RNA interference vector.

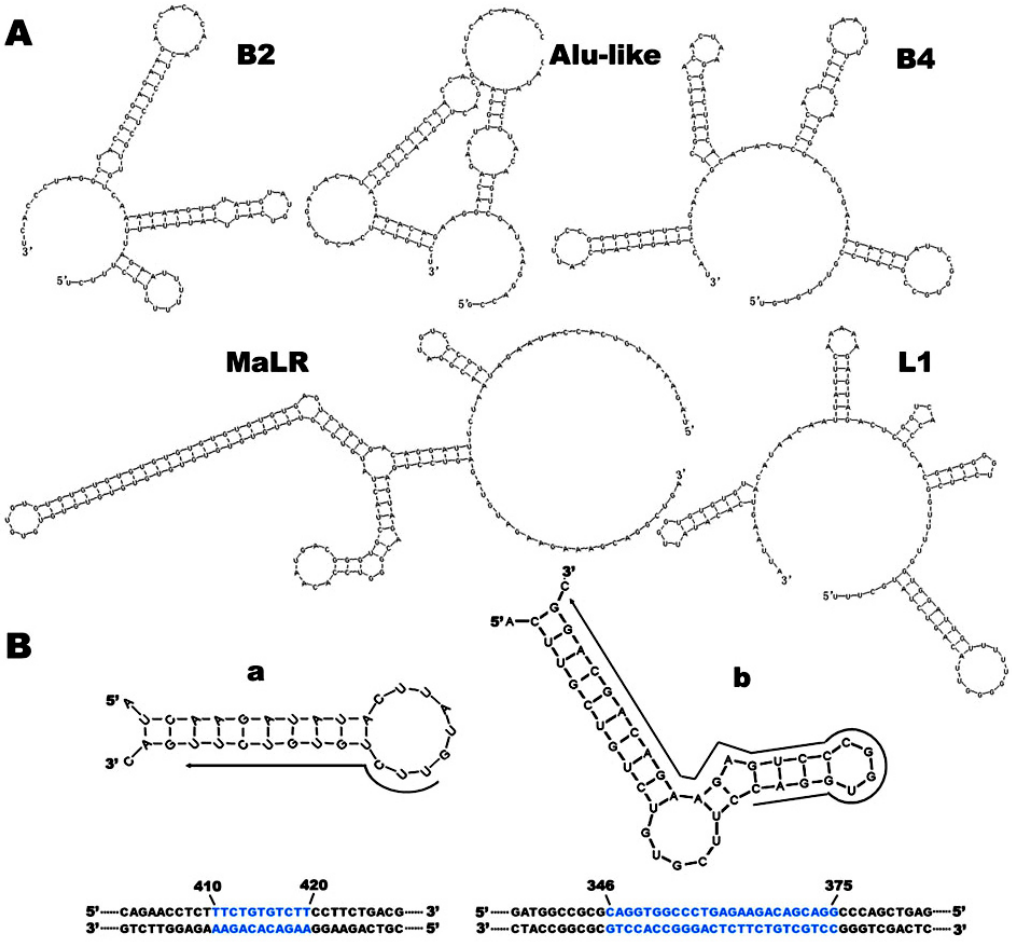

Figure 6. Intron miRNA analysis. Intron sequences within mouse *dmrt1* genomic BAC clone AC132140 were used for search for repeat sequences, their secondary structures (A) and possible complementary regions with *dmrt1* mRNA (B). MaLR, L1, Alu-like, B2 and B4 represent five kinds of repeat families. miRNAs targeting relevant *dmrt1* were shown in lower panel. The numbers on the sequences indicate hybridization positions at *dmrt1d* isoform mRNA.

5. DISCUSSION

Although RNAi silences gene expression in a sequence-specific manner, several recent studies have suggested that the specificity of silencing is not absolute. Indeed miRNAs downregulate a greater number of transcripts than previously appreciated (23). Because the imprecise base pairs between the typical miRNA and a target mRNA, and any given miRNA can bind to a broad spectrum of different mRNAs, this raises questions and concerns, how precisely recognising between miRNA and mRNA and how enormous regulatory potential of miRNA. Target recognition of siRNA is far more degenerative than previously considered (27). Several mutational studies showed the primacy of critical base pairs and base-pairing patterns involving the first nine nucleotides of the miRNA (23, 28-30). We show here that the mutation significantly changed kinetics of the folding and unfolding of secondary structures and decreased *Tm* value of the duplex melting. Because of its thermodynamic unstability, the mutant duplex will spatially affect its binding to PAZ domain of the Dicer for RNA silencing pathway. Crystal structure analysis has shown that in a sequence-independent manner, PAZ anchors the 2-nucleotide 3'overhang of the siRNA duplex within a highly conserved binding pocket, and secures the duplex by binding the 7-nucleotide phosphodiester backbone of the overhang-containing strand and capping the 5'-terminal residue of the complementary strand (19). Generally nuclear excising of pri-miRNAs by Drosha introduces a stem-loop duplex with a 2-nt 3' overhang at the cleavage site for Dicer processing further in the cytoplasm. However further studies are needed to understand precise interactions between dsRNA and Drosha and also Dicer, and therefore their recognition events for a variety of different target mRNAs in the RNA silencing pathway.

According to their origin or function, three types of naturally occurring small RNA have been described: short interfering RNAs (siRNAs), repeat-associated short interfering RNAs (rasiRNAs) and microRNAs (miRNAs). dsRNAs produced by hybridization of overlapping transcripts such as repetitive sequences and spliced introns are a new class of small non-coding regulatory elements. These transcripts containing complementary inverted repeats fold back on themselves to form dsRNA hairpins. Indeed, intron-derived miRNAs have been found in *C. elegans*, mouse, and human (31), which will be an alternative pathway for miRNA biogenesis. Because of the complex regulatory mechanisms of endogenous *dmrt1* in gonadal development, we searched for the possible RNA interfering forms, especially intronic miRNA structures of mouse *dmrt1* gene. We observed that within *dmrt1* introns, there were 174 repeat elements which may fold back to form hairpin secondary structures. Figure 6 shows five typic folding structures (Figure 6A). Some spliced intron elements during transcription may also directly target against mRNA. Indeed, we observed possible 29 duplexes targeting against *dmrt1* mRNA and two of them were shown in Figure 6B. We show here many of this kind of dsRNA hairpins in mouse *dmrt1* gene, and while some of them target directly against *dmrt1* mRNA, most of them may join in expression regulation of the other genes in the *dmrt1* cascade. Further studies on this kind of gene regulation will help in understanding RNA functions and sexual development.

6. SIGNIFICANCE

Short interfering RNA mutation significantly changed kinetics of the folding and unfolding of secondary structures and decreased *Tm* value of the duplex melting. The mutant duplex was more unstable thermodynamically than the normal structure. Mutants targeting mouse *dmrt1* affected knockdown effects of the gene by the RNA interference in both transfected cells and endogenous Sertoli cells. These findings will undoubtedly help in further understanding RNA silence in vertebrate development and drug design for target gene.

7. ACKNOWLEDGMENT

The work was supported by the National Natural Science Foundation of China, the National Key Basic Research project, the Program for New Century Excellent Talents in University and the Key Project of Chinese Ministry of Education (No. 2004.28). There is not any financial conflict of interest.

8. REFERENCES

1. Brennecke, J., D. R. Hipfner, A. Stark, R. B. Russell & S. M. Cohen: bantam encodes a developmentally regulated microRNA that controls cell proliferation and regulates the proapoptotic gene hid in Drosophila. *Cell*, 113, 25-36 (2003)

2. Xu, P., S. Y. Vernooy, M. Guo & B. A. Hay: The Drosophila microRNA Mir-14 suppresses cell death and is required for normal fat metabolism. *Curr Biol*, 13, 790-5 (2003)

3. Poy, M. N., L. Eliasson, J. Krutzfeldt, S. Kuwajima, X. Ma, P. E. Macdonald, S. Pfeffer, T. Tuschl, N. Rajewsky, P. Rorsman & M. Stoffel: A pancreatic islet-specific microRNA regulates insulin secretion. *Nature*, 432, 226-30 (2004)

4. Calin, G. A., C. D. Dumitru, M. Shimizu, R. Bichi, S. Zupo, E. Noch, H. Aldler, S. Rattan, M. Keating, K. Rai, L. Rassenti, T. Kipps, M. Negrini, F. Bullrich & C. M. Croce: Frequent deletions and down-regulation of micro- RNA genes miR15 and miR16 at 13q14 in chronic lymphocytic leukemia. *Proc Natl Acad Sci U S A*, 99, 15524-9 (2002)

5. Calin, G. A., C. Sevignani, C. D. Dumitru, T. Hyslop, E. Noch, S. Yendamuri, M. Shimizu, S. Rattan, F. Bullrich, M. Negrini & C. M. Croce: Human microRNA genes are frequently located at fragile sites and genomic regions involved in cancers. *Proc Natl Acad Sci U S A*, 101, 2999-3004 (2004)

6. Chen, C. Z., L. Li, H. F. Lodish & D. P. Bartel: MicroRNAs modulate hematopoietic lineage differentiation. *Science*, 303, 83-6 (2004)

7. Lee, R. C., R. L. Feinbaum & V. Ambros: The C. elegans heterochronic gene lin-4 encodes small RNAs with antisense complementarity to lin-14. *Cell*, 75, 843-54 (1993)

8. Giraldez, A. J., R. M. Cinalli, M. E. Glasner, A. J. Enright, J. M. Thomson, S. Baskerville, S. M. Hammond, D. P. Bartel & A. F. Schier: MicroRNAs regulate brain morphogenesis in zebrafish. *Science*, 308, 833-8 (2005)
9. Bartel, D. P.: MicroRNAs: genomics, biogenesis, mechanism, and function. *Cell*, 116, 281-97 (2004)
10. Bentwich, I., A. Avniel, Y. Karov, R. Aharonov, S. Gilad, O. Barad, A. Barzilai, P. Einat, U. Einav, E. Meiri, E. Sharon, Y. Spector & Z. Bentwich: Identification of hundreds of conserved and nonconserved human microRNAs. *Nat Genet*, 37, 766-70 (2005)
11. Lim, L. P., M. E. Glasner, S. Yekta, C. B. Burge & D. P. Bartel: Vertebrate microRNA genes. *Science*, 299, 1540 (2003)
12. Meister, G. & T. Tuschl: Mechanisms of gene silencing by double-stranded RNA. *Nature*, 431, 343-9 (2004)
13. Cullen, B. R.: Transcription and processing of human microRNA precursors. *Mol Cell*, 16, 861-5 (2004)
14. Hannon, G. J. & J. J. Rossi: Unlocking the potential of the human genome with RNA interference. *Nature*, 431, 371-8 (2004)
15. Ambros, V.: The functions of animal microRNAs. *Nature*, 431, 350-5 (2004)
16. Mello, C. C. & D. Conte, Jr.: Revealing the world of RNA interference. *Nature*, 431, 338-42 (2004)
17. Ding, S. W.: RNAi: Mechanisms, biology and applications. *FEBS Lett*, 579, 5821 (2005)
18. Yan, K. S., S. Yan, A. Farooq, A. Han, L. Zeng & M. M. Zhou: Structure and conserved RNA binding of the PAZ domain. *Nature*, 426, 468-74 (2003)
19. Ma, J. B., K. Ye & D. J. Patel: Structural basis for overhang-specific small interfering RNA recognition by the PAZ domain. *Nature*, 429, 318-22 (2004)
20. Pham, J. W., J. L. Pellino, Y. S. Lee, R. W. Carthew & E. J. Sontheimer: A Dicer-2-dependent 80s complex cleaves targeted mRNAs during RNAi in Drosophila. *Cell*, 117, 83-94 (2004)
21. Nykanen, A., B. Haley & P. D. Zamore: ATP requirements and small interfering RNA structure in the RNA interference pathway. *Cell*, 107, 309-21 (2001)
22. Tomari, Y., T. Du, B. Haley, D. S. Schwarz, R. Bennett, H. A. Cook, B. S. Koppetsch, W. E. Theurkauf & P. D. Zamore: RISC assembly defects in the Drosophila RNAi mutant armitage. *Cell*, 116, 831-41 (2004)
23. Lim, L. P., N. C. Lau, P. Garrett-Engele, A. Grimson, J. M. Schelter, J. Castle, D. P. Bartel, P. S. Linsley & J. M. Johnson: Microarray analysis shows that some microRNAs downregulate large numbers of target mRNAs. *Nature*, 433, 769-73 (2005)
24. Germann, M. W., B. W. Kalisch, R. T. Pon & J. H. van de Sande: Length-dependent formation of parallel-stranded DNA in alternating AT segments. *Biochemistry*, 29, 9426-32 (1990)
25. Zhao, Y., Z. Y. Kan, Z. X. Zeng, Y. H. Hao, H. Chen & Z. Tan: Determining the folding and unfolding rate constants of nucleic acids by biosensor. Application to telomere G-quadruplex. *J Am Chem Soc*, 126, 13255-64 (2004)
26. Karl, A. F. & M. D. Griswold: Sertoli cells of the testis: preparation of cell cultures and effects of retinoids. *Methods Enzymol*, 190, 71-5 (1990)
27. Du, Q., H. Thonberg, J. Wang, C. Wahlestedt & Z. Liang: A systematic analysis of the silencing effects of an active siRNA at all single-nucleotide mismatched target sites. *Nucleic Acids Res*, 33, 1671-7 (2005)
28. Kiriakidou, M., P. T. Nelson, A. Kouranov, P. Fitziev, C. Bouyioukos, Z. Mourelatos & A. Hatzigeorgiou: A combined computational-experimental approach predicts human microRNA targets. *Genes Dev*, 18, 1165-78 (2004)
29. Vella, M. C., E. Y. Choi, S. Y. Lin, K. Reinert & F. J. Slack: The C. elegans microRNA let-7 binds to imperfect let-7 complementary sites from the lin-41 3'UTR. *Genes Dev*, 18, 132-7 (2004)
30. Doench, J. G. & P. A. Sharp: Specificity of microRNA target selection in translational repression. *Genes Dev*, 18, 504-11 (2004)
31. Ying, S. Y. & S. L. Lin: Intronic microRNAs. *Biochem Biophys Res Commun*, 326, 515-20 (2005)

Key Words: Thermodynamics, Folding, RNA interference, *dmrt1*, Sertoli cells

Send correspondence to: Dr Rongjia Zhou and Hanhua Cheng, Department of Genetics and Center for Developmental Biology, College of Life Sciences, Wuhan University, Wuhan 430072, P. R. China, Tel: 0086-27-68756253, Fax: 0086-27-68756253, E-mail: rjzhou@whu.edu.cn, hhcheng@whu.edu.cn

http://www.bioscience.org/current/vol11.htm